Porosity determination with standard well-logging data: implications for the local fluid flow regime of Mauna Kea Lava Flows (HSDP-2)

A. Buysch; R. Pechnig (Applied Geophysics, RWTH Aachen, Lochnerstraße 4-20, 52056 Aachen, Germany; email: A.Buysch@geophysik.rwth-aachen.de); U. Harms (GFZ Potsdam, Telegrafenberg, 14473 Potsdam, Germany; email: Ulrich@gfz-potsdam.de).

1. Introduction

One of the objectives of our studies in the 'Hawaii Scientific Drilling Project HSDP-2' is to understand the local fluid flow regime on the basis of logging data. Usually, petrophysical measurements for bulk porosity in combination with density measurements are referred to as an indicator for possible permeable zones, so-called fluid pathway zones. These data have not been measured in HSDP-2 due to environmental and permitting reasons. Hence, the acquired resistivity and velocity measurements were used to investigate fluid activities. On the basis of existing porosity estimates of crystalline as well as sedimentary rocks, we have developed a porosity profile derived from downhole resistivity measurements. This was applied to estimate the propagation of possible fluid pathway zones and to contribute to our interpretations of the genetic evolution of the whole volcano system on the basis of log interpretation.

2. Lithological classification on the basis of petrophysical characteristics

The geophysical measurements (Fig. 1) indicate a subdivision of the logged profile into nine large scale sections, named Log Units (LU 1 – 9). For the petrophysical properties the log units show remarkable changes within and between each unit. This can be summarized as following: beside an expected resistivity increase with depth due to an increasing consolidation, the log data exhibit various unexpected petrophysical effects (Fig. 2), which can be related to deviating changes caused by primary and secondary evolution. Regarding its implications on overall porosity and influence on local fluid flow, resistivity measurements lead to a different consideration of formerly similar interpreted rock types. In the following, we present a more detailed description of the log units:

- *Log Unit 1* contains subaerial lava flow successions (mainly Aa and Pahoehoe) with low resistivity values and large variations in gamma-ray values; the low resistivity values give hint to an overall high porosity for the entire section. The high standard deviation of the gamma-ray log values is caused by large variations in all three spectrally measured elements (K, U, Th), which is indicative for secondary weathering and alteration of the subaerial flows.

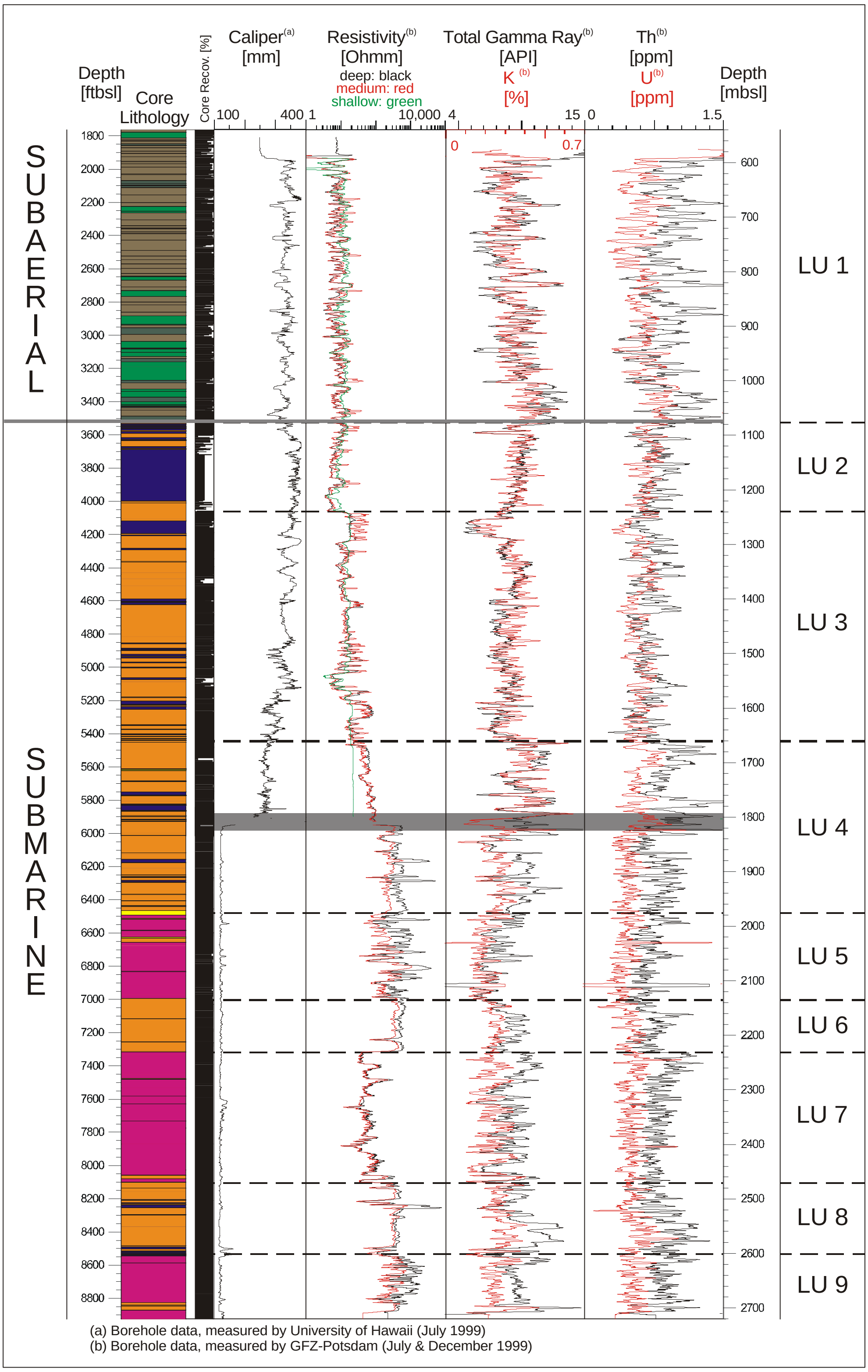

Fig. 1: *The logging data allow for subdivision of the HSDP-2 profile into nine large-scaled log units (LU 1 – 9), differing in their petrophysical characteristics. The log unit boundaries partly correspond to changes in the core lithology. The use of different resistivity tools require a separation of the statistical calculation in LU 4 (thick grey line).*

- *Log Unit 2* separates the uppermost part of the submarine section. The lowest resistivity values of the entire section were measured in this log unit. This points to a high proportion of unconsolidated material, and thus influences the porosity estimation. Moreover, the log responses indicate an overestimation of massive units in the core profile. This is consistent with high core losses in this borehole section caused by the occurrence of rubble material.

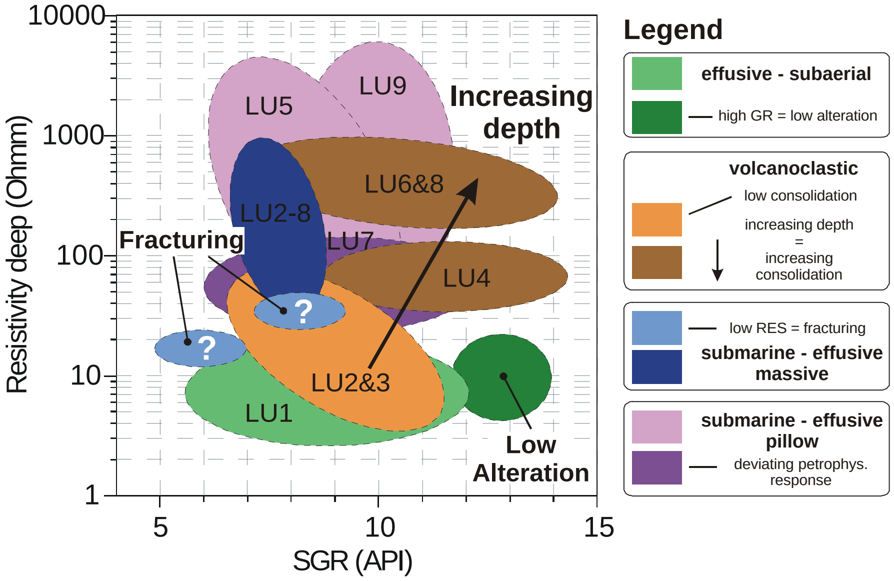

Fig. 2: *Scatter plot of resistivity data (deep induction) and spectral gamma-ray activity (SGR); the plot results from the subdivision of the data according to the petrophysical response in the nine Log Units (LU 1-9). The increasing consolidation with depth is indicated by an arrow.*

- *Log Unit 3* exhibit homogeneous submarine units on the first view composed of hyaloclastites with frequent intercalations of massive basalt units. The significant increase in resistivity compared to LU 2 points to stronger consolidation of the drilled volcanoclastics, which is consistent with observations on core material.
- *Log Unit 4* is characterized by a second increase in resistivity compared to the overlying submarine formations. The jump in resistivity at the LU 3 / LU 4 boundary marks a significant change within the hyaloclastite series and indicates a rapid increase in consolidation and cementation of the volcanoclastic material. An additional change of gamma-ray activity to higher values and an increasing standard deviation might reveal the influence of cementing fluids on formerly porous media.
- *Log Units 5, 7 & 9* are Pillow units with low readings in spectral gamma-ray and resistivity logs. Latter points to a higher porosity than in the surrounding hyaloclastic units, reflecting in combination with a large scatter of the sonic velocity logs a strong fracturing of the basalts. The lowest average values of resistivity and sonic velocity logs are observed in LU 7, caused by fracturing but also by the high vesicularity of this log unit.
- *Log Units 6 & 8* represent homogenous and strongly consolidated hyaloclastic series with log responses comparable to those of LU 4.

3. Preliminary porosity calculation

We applied the Archie equation (Archie, 1942) on the resistivity measurements with Archie standard coefficients *a* = *1* and *m* = *2*, to get a first impression of the amount of porosity in the HSDP-2 drillhole. The use of these coefficients has turned out to be an adequate method for preliminary estimations of porosity in basaltic rocks (e.g. Frese, 1999). The results of porosity calculations are compared with core derived porosity (Dannowski and Huenges, 2000), and displayed as log plot data (Fig. 3) and box plot diagram data (Fig. 4).

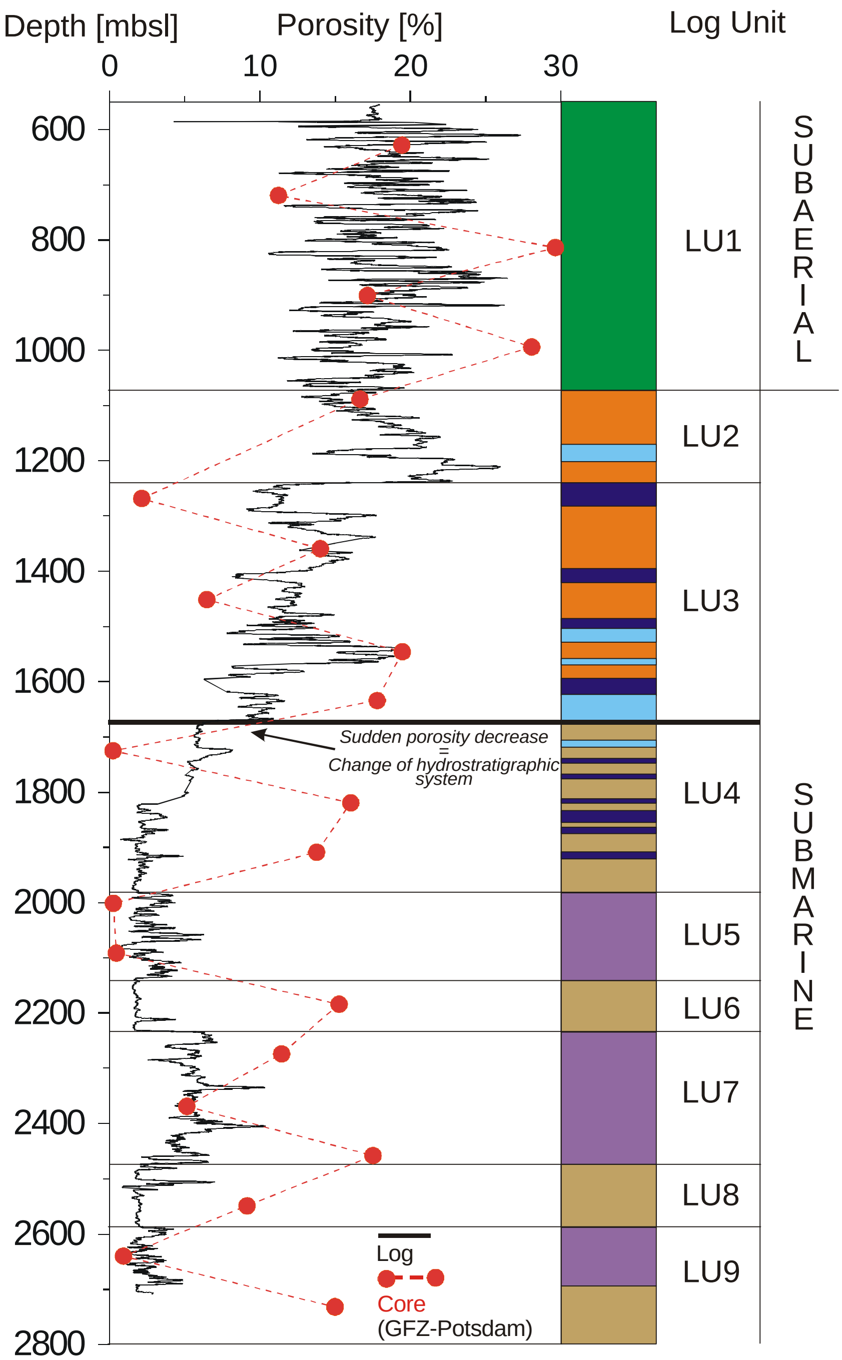

Fig. 3: *Comparison of porosity data from HSDP-2 drillhole as calculated from resistivity log by Archie equation and porosity determined on core samples. Diverting porosity values from subaerial to submarine lava flows indicate large differences between whole-rock in-situ, and core measurements. Possible reasons are lithological differences, but also core procedure related causes, e.g. preferred selection, pressure release and drilling induced weakness.*

Although the basic rock type is composed of basaltic lava flows in general, many diverting effects in porosity can be expected due to the totally different morphological characteristics. Figure 5 shows possible morphological differences as taken from core pictures; the idealized pictures refer to the possible pore structure derived from cores. The large differences between log derived porosity and core porosity (Fig. 4) emphasize the strong influence of basaltic rock morphology on porosity determinations.

In the subaerial part data sets from log and core investigations show a large scatter, but cover a more or less comparable range of values. Strong brecciation and vesicularity at the top and bottom of flows is the controlling factor for rock porosity, thus leading to an overall porosity of F_{log} = 10 – 25 % (Fig. 4). This seems to be in agreement with core measurements showing values in a range of F_{core} = 5 – 30 % (max. F_{core} = 52 %). However, the controlling factor for an effective porosity with redundant fluid flow is not only the presence of vesicular parts in subaerial lava flows but also the conductivity between porosity.

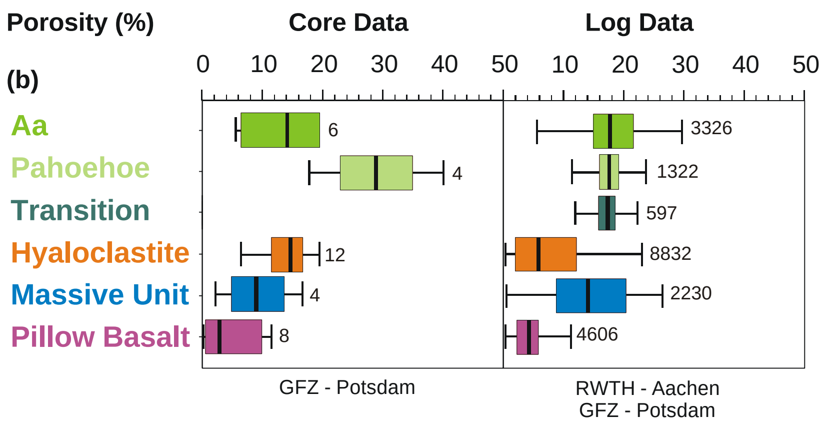

Fig. 4: *Box plot diagram of log and core porosity (see also Fig. 4); the comparison emphasizes the large differences between core and log measurements, esp. for hyaloclastites and massive units. Furthermore, the large standard deviation of log porosity for these rock types implicates a re-definition in accordance to their secondary evolution.*

Significant differences between log and core porosity occur in the submarine section. These differences might be attributed to different factors: (1) to inadequate Archie parameters; (2) to a predominant selection of coherent, unfractured material for core analyses, and (3) to an effect of decreasing stability and coherence of core material, due to decompression and further investigations after drilling. The second issue might be addressed within the Pillow sections, where the log porosities are higher, representing massive as well as fractured Pillow sections, while the core samples with lower porosities are preferably taken from massive coherent parts. A similar difference between core and log porosity is also observed in Pillow series from the upper oceanic crust. In contrast, core porosities of the hyaloclastic series exhibit on average higher porosities than those derived from the in-situ log data. The third issue seems to be the most reasonable which is not so surprising, taking into account the very young age (less than a few 100 Ka; DePaolo et al., 2001) of compaction and cementation .

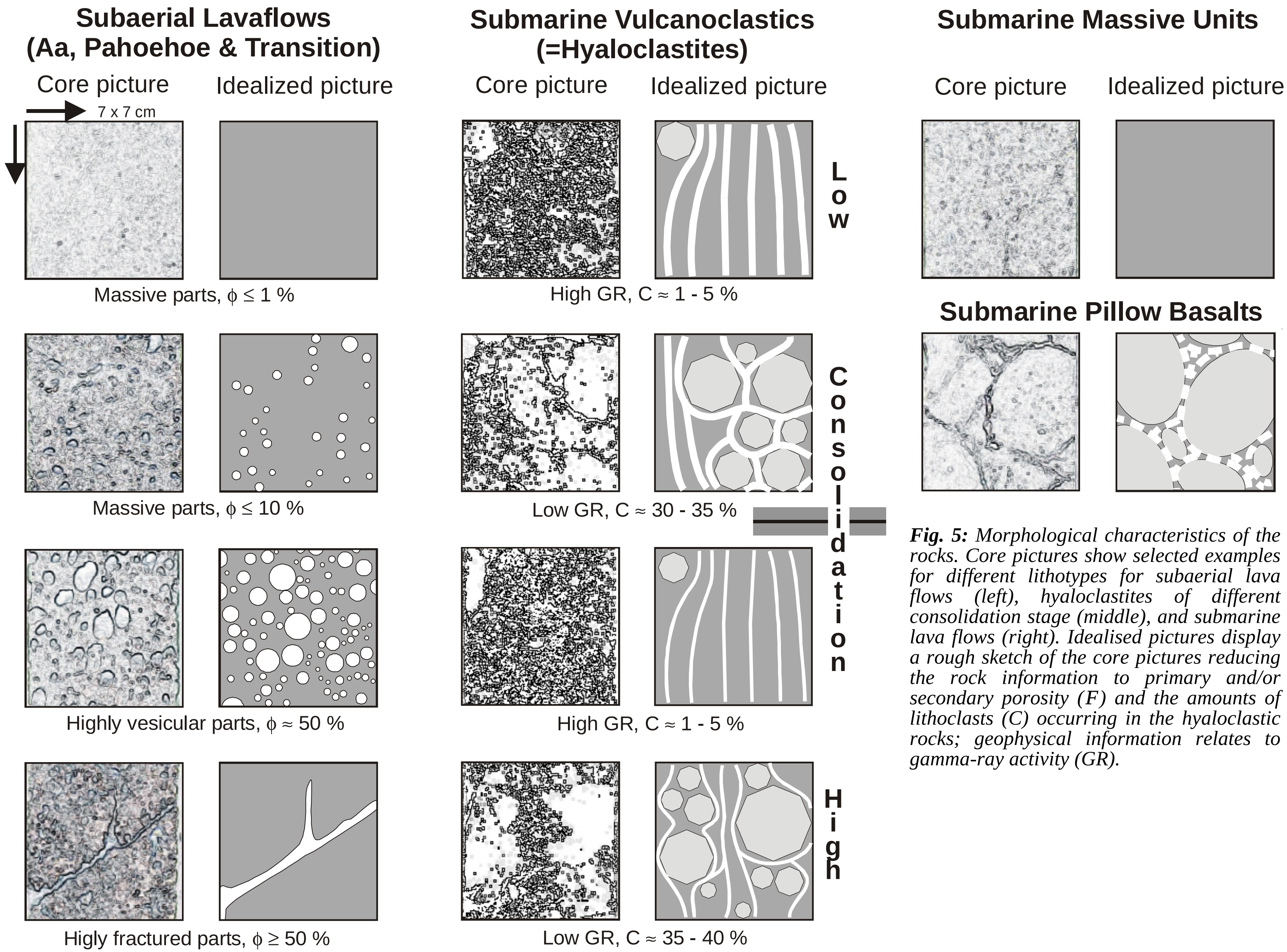

Fig. 5: *Morphological characteristics of the rocks. Core pictures show selected examples for different lithotypes for subaerial lava flows (left), hyaloclastites of different consolidation stage (middle), and submarine lava flows (right). Idealised pictures display a rough sketch of the core pictures reducing the rock information to primary and/or secondary porosity (F) and the amounts of lithoclasts (C) occurring in the hyaloclastic rocks; geophysical information relates to gamma-ray activity (GR).*

Even considering uncertainties due to the inaccurate knowledge of the Archie parameters, the log derived porosity profile provides important information to the large scale hydrogeological situation of Mauna Kea. The observed stepwise decrease in log porosity within the hyaloclastites from LU 2 to LU 8 can be related to different stages of compaction and cementation. The log data depict also very clearly the extension of hydraulic zones, e.g. a prominent hydrostratigraphic boundary between 1560 – 1660 mbsl (so called '1600-boundary'). This border corresponds to a decrease in porosity from F_{log} = 15 – 20 % to F_{log} = 5 % and a significant temperature increase (Dannowski and Huenges, 2000). This is probably generated by two effects: a thick massive unit occurring in this depth interval and the uppermost limitation of the cementation front within the hyaloclastites at a slightly lower depth. Moreover, it implies a significant change of the hydrogeological situation above and below the 1650 m - boundary: above this barrier hyaloclastites with porosities F_{hyalo} = 12 – 25 % mainly serve as possible fluid pathway zones, whereas the effusives (here: massive units) have lower porosity ($F_{massive}$ = 7 – 12 %) and function as barriers. Below this depth distinct low velocity/low resistivity zones corresponding to fractures in (Pillow)-basalts serve as fluid transport pathways. Effusives (here: Pillow basalts) exhibit higher porosity F_{Pillow} = 2 – 10 % than hyaloclastites $F_{hyalo} \approx 2$ % and therefore act as fluid conductors.

4. Implications on local fluid flow

Beside the general primary evolution of the volcano – from the submarine stage, over a subaerial build-up and finally subsidence to its present stage (Buysch et al., subm.) – the post-depositional era has much influence on the volcanic edifice of Mauna Kea. Sudden changes in porosity, despite a general decrease tendency towards depth (Fig. 6), show that the fluid flow regime is not only controlled by the primary lithology but also by a secondary impregnation of the rocks due to cementation and alteration processes. On the contrary, the ancient and the present complex fluid flow regimes in Mauna Kea with its interlayering aquifers series from different sources (ocean and groundwater; Paillet and Thomas, 1996; Thomas et al., 1996) control the evolution of secondary assemblages.

Our investigations favour the following evolution of the local fluid flow regime with time (Fig. 6):

- First impacts of oceanic fluids occurred directly after flow emplacement during an early phase of submarine stage; the low compaction grade allowed fluid flow in all parts of the formations (Pillow units and hyaloclastites); increasing consolidation and cementation of hyaloclastites directed the fluid flow to the Pillow units, as size, amount, and connectivity of vesicles and/or fractures were the controlling factor.

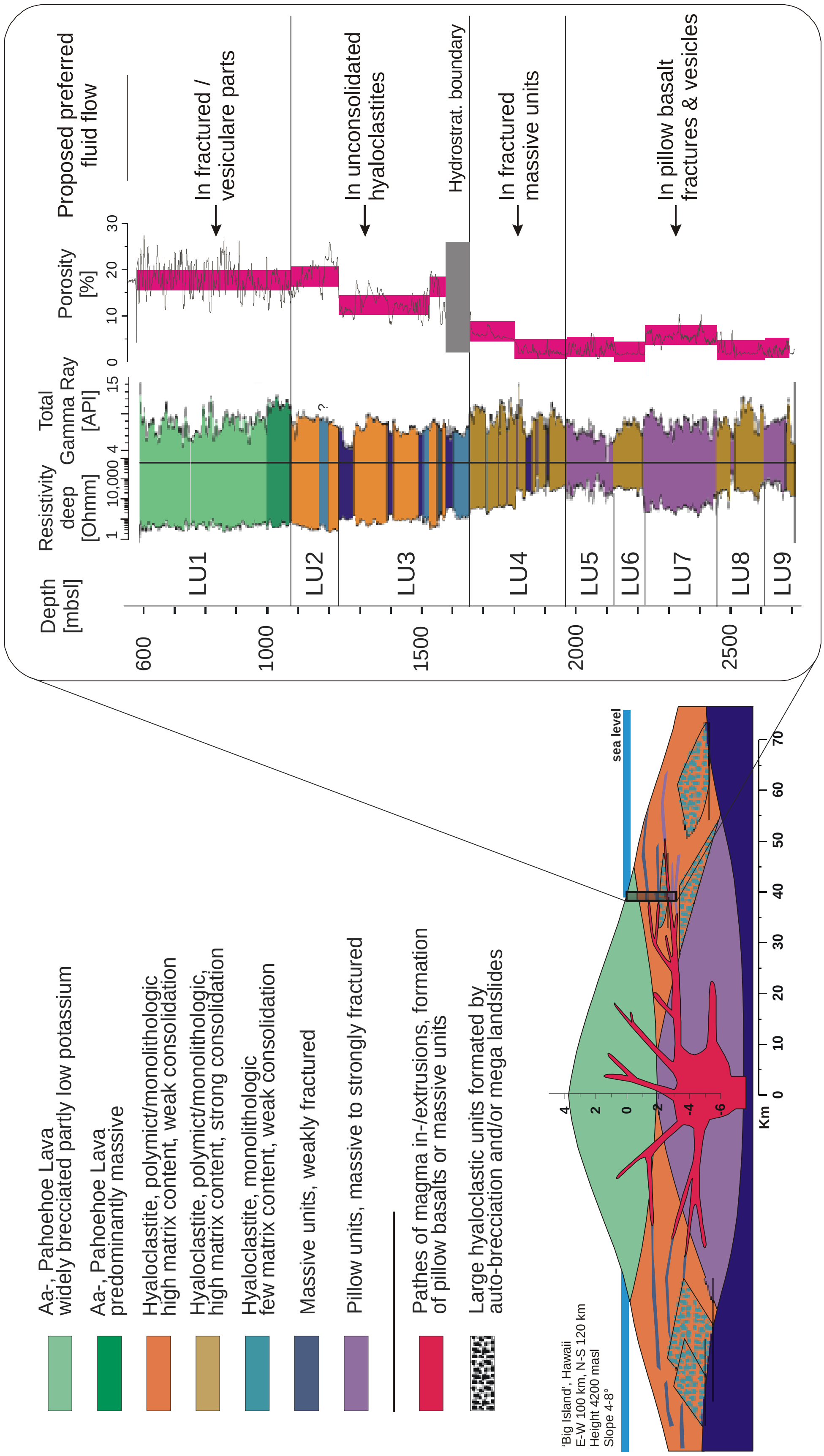

Fig. 6: *Generalized lithological profile deduced from log responses and compared with a preliminary porosity profile as well as the proposed fluid flow pathways in accordance to the occurring rock type (right). The information is integrated into a structure model of the volcano (left; modified after DePaolo et al., 2001).*

- Further build-up of the volcano and subsequent consolidation lead to the evolution of a hydrostratigraphic boundary (1600–boundary; Buysch et al., subm.), which is indicative for a change in general flow regime; porous formations of similar rock types show different flow behaviour above and below this boundary (see 'Preliminary porosity calculation').
- Fluid circulation along distinct flow parts (e.g. altered and brecciated intervals) and lava tubes of subaerial lava flows generated the formation of fluid pathway zones with corresponding alteration type. This type is mainly initiated by an intense weathering of vesicular and brecciated flow tops and bottoms, often leading to soil formation, and loss of mobile elements, e.g. potassium (Mathe et al., 1999). A deviating area with high gamma ray activity in the bottom part (1006 – 1079 mbsl) seems to be less influenced by weathering, pointing to different fluid flow mechanisms compared to the rest of the subaerial stage.

General differences between subaerial and submarine stages can be summarized as following: The lava flows are subject to a break-up of rock coherence, especially, in the vesicular and brecciated flow parts of the subaerial stage. Formerly vesicular parts tend to be affected by alteration in that way, that more conductivity for fluids is caused and again further alteration is favoured. In contrast, the more coherent rock appearance of submarine rocks (e.g. massive units) with low vesicularity in general refines a cementation effect of alteration related fluid flow and leads to a certain barrier effect for subsequent fluid flow.

5. References

Archie, G.E., The electrical resistivity log as an aid in determining some reservoir characteristics, Pet. Tech., 5, 1-8, 1942.

Buysch, A., R. Pechnig and U. Harms, Evolution scenarios for Mauna Kea volcano deduced from geophysical downhole measurements, *Geochemistry, Geophysics, Geosystems, submitted*, 2002.

Dannowski G. and E. Huenges, Continuous Temperature Observations in the Hawaii NSF/ICDP Borehole First Results and Models. AGU Fall Meeting. December 15.-19. 2000. San Francisco, *Eos Trans.* AGU, 81, 48 Fall Meet. Suppl., V21A-08, 2000.

DePaolo, D.J., E. Stolper and D. Thomas, Deep Drilling into a Hawaiian volcano, *Eos Trans.* AGU, 82, 13, 151-155, 2001.

Frese, D., Standardverfahren zur Porositätsberechnung aus geophysikalischen Bohrlochmessungen - Ein Vergleich für Lithologien kontinentaler und ozeanischer Kruste, *master thesis, unpublished*, RWTH Aachen, 1998.

Mathe P.E., P. Rochette, D. Van Damme and F. Colin, Volumetric changes in weathered profiles: iso-element mass balance method questioned by magnetic fabric, *Earth Planet Sci. Lett*., 167, 255-267, 1999.

Paillet, F.L. and D.M. Thomas, Hydrology of the Hawaii Scientific Drilling Project KP-1, 1, Hydraulic conditions adjacent to the well bore, *J. Geophys. Res.*, 101, B5, 11675-11682, 1996.

Thomas, D. M., F.L. Paillet and M.E. Conrad, Hydrogeology of the Hawaii Scientific Drilling Project borehole KP-1, 2, Groundwater chemistry and regional flow patterns, *J. Geophys. Res.*, 101, B5, 11683-11694, 1996.